J. Phys. B: At. Mol. Opt. Phys. **26** (1993) L97–L102. Printed in the UK

LETTER TO THE EDITOR

Three-electron radiative transitions

A Ehresmann†, V A Kilin†‖, L V Chernysheva†¶, H Schmoranzer†, M Ya Amusia‡* and K-H Schartner§

† Fachbereich Physik, Universität Kaiserslautern, D-6750 Kaiserlautern, Federal Republic of Germany

‡ Institut für Theoretische Physik, Johann-Wolfgang-Goethe-Universität, D-6000 Frankfurt/M 11, Federal Republic of Germany

§ I Physikalisches Institut, Justus-Liebig-Universität, D-6300 Giessen, Federal Republic of Germany

Received 18 November 1992

Abstract. A new type of many-electron radiative transitions involving three electrons is predicted. The results of their investigation by many-body perturbation theory are presented. New spectral lines observed in the wavelength range of 37.5 to 54.0 nm by means of photon-induced fluorescence spectroscopy (PIFS) following the excitation of the Kr I $3d^{-1}np$ resonances are reported and compared with the predictions.

The first observation of a single-photon decay of double-vacancy states was reported by Woelfli *et al* (1975). In the theoretical explanation by Amusia *et al* (1977a, b), the $1s^{-2}$ double-vacancy state, e.g., decays into $ns^{-1}mp^{-1}$ states by emission of a single photon. These radiative transitions are allowed by the parity changing law, whereas transitions into $np^{-1}mp^{-1}$ states are forbidden. If, however, a more complicated initial state is considered with an additional excited electron, the latter can change its orbital momentum without noticeable alteration of its energy, thus opening many channels of a single-photon double-vacancy decay.

The aim of this letter is to present the results of the first investigation of the single-photon decay of double-vacancy-one-electron states in the lowest non-vanishing order of perturbation theory, including calculated transition probabilities. This process is really a many-particle one, because at least three electrons actively participate in it, two of them filling the initially vacant states, while the third one alters its orbital momentum. Therefore these transitions will be called in this letter 'three-electron radiative transitions' (TERT).

The interest in TERT is amplified by recent experimental observations (Ehresmann *et al* 1992). Using the photon-induced fluorescence spectroscopy (PIFS) method (see, e.g., Schartner *et al* 1990), a new group of weak lines was observed in the wavelength region between 540 Å and 375 Å (26.3–32.8 eV) after resonant excitation of the Kr I $3d^{-1}np$ ($n = 5, 6$) states. Two example spectra of the Kr I $3d_{5/2}^{-1}5p$ (at 91.2 eV) and the Kr I $3d_{3/2}^{-1}5p$ resonances (at 92.43 eV) are shown in figure 1 together with a spectrum

‖ Permanent address: Department of Mathematics-1, Tomsk Polytechnic University, 634004 Tomsk, Russia.

¶ Permanent address: Institute for Informatics and Automation of the Academy of Science, 199178 St Petersburg, Russia.

* Permanent address: A F Ioffe Physical Technical Institute of the Academy of Science, St Petersburg, Russia.

0953-4075/93/050097+06$07.50

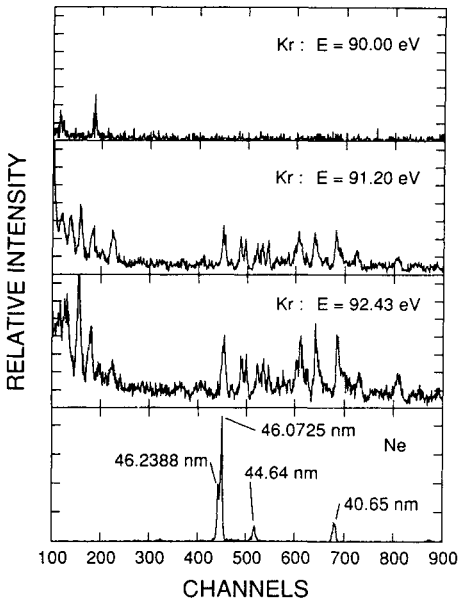

Figure 1. Experimental PIFS spectra of Kr recorded at different excitation energies in the fluorescence wavelength region between 36 nm and 54 nm. 90.00 eV, below the $3d^{-1}np$ resonances; 91.20 eV, $3d_{5/2}^{-1}5p$ resonance; 92.43 eV, $3d_{3/2}^{-1}5p$ resonance. The spectra taken at the resonances have not been normalized. The Ne spectrum was used for the wavelength calibration.

below the resonances (at 90.00 eV). Additionally a Ne spectrum is shown, recorded with the same experimental parameters, which was used for wavelength calibration. The observed photon energies are close to the energy difference of Kr II $4s^{-2}np$ and $4p^{-2}n'l'$ states. The former ones are easily populated by Auger decay of the $3d^{-1}np$ resonance. Thus, additionally to general formulae obtained in the lowest order of perturbation theory for the transition probabilities, the following specific example of TERT $4s^{-2}np \rightarrow 4p^{-2}n'l' + \gamma$ ($n'l' = n$'s, n'd, including $n' = n$) will be considered as a tentative explanation of the new lines. Calculations were performed using the computer codes ATOM (Amusia and Chernysheva 1983).

Let us consider the radiative transition from the ion state with two holes i_1, i_2 and an electron excited to a discrete level n to another double-hole (f_1f_2)-one-electron (n') state, i.e. the transition $i_1i_2n \rightarrow f_1f_2n' + \gamma$. Within the dipole and LS-coupling approximations the probability of the radiative transition is defined by the expression†

$$W = \frac{\alpha^3\omega^3}{(2L+1)(2S+1)} \sum_{MM'M_sM_s'} |A|^2 \delta(E_i - E_f - \omega) \tag{1}$$

where $\alpha = \frac{1}{137}$ is the fine structure constant, $\omega = E_i - E_f$ is the energy of the emitted photon, E_i and E_f are the initial and final state energies, while A is the amplitude of the dipole transition

$$A = \langle i_1 i_2 [L_i S_i] n [LMSM_s] | \boldsymbol{D} | f_1 f_2 [L_f S_f] n' [L'M'S'M_s'] \rangle. \tag{2}$$

† Atomic units are used, $e = \hbar = m = 1$.

Here L and S are the orbital momentum and spin with projections M and M_s, respectively, and $\boldsymbol{D}$ is the dipole operator.

Since three electrons change their states, the lowest non-vanishing order perturbation theory diagrams, describing TERT, must include at least two wavy lines of the Coulomb interelectron interaction, see e.g. figure 2 (the usual many-body theory diagram notations are used: the line with an arrow to the left is a vacancy, the double-arrow line denotes a discrete electron excitation, while the broken line stands for a photon). In this letter only those transitions $i_1 i_2 n \to f_1 f_2 n' + \gamma$ will be considered which are allowed due to an active participation of the excited electron n at least by changing its orbital momentum. Thus, the three-electron nature of the above transitions is evident.

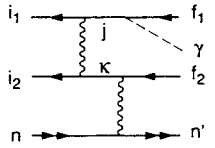

Figure 2. Typical TERT perturbation-theory diagram (Feynman diagram).

The analytical expression of the partial amplitude, corresponding to the diagram in figure 2, reads

$$A = \sum_k \sum_j \frac{\langle i_1 i_2|u|jk\rangle\langle kn'|u|f_2 n\rangle\langle j|\boldsymbol{D}|f_1\rangle}{(\varepsilon_{i_1}+\varepsilon_{i_2}-\varepsilon_j-\varepsilon_k)(\varepsilon_j-\varepsilon_{f_1}+\omega)} \tag{3}$$

and includes not only the summation over intermediate k-, j-vacancy states, but also the summation over discrete excited (integration over continuum) electron states. In equation (3), $\langle kl|u|mn\rangle = \langle kl|r_{12}^{-1}|mn\rangle - \langle kl|r_{12}^{-1}|nm\rangle$ is the difference between direct and exchange Coulomb matrix elements, $\langle k|\boldsymbol{D}|l\rangle$ is the dipole matrix element, ε are the Hartree–Fock (HF) one-electron energies.

Even in the lowest order of perturbation theory, a number of diagrams (partial amplitudes) similar to figure 2 contribute to the total amplitude under consideration because, additionally to the different variations of one-electron states involved in the TERT, the photon (broken line) could be emitted from any of the vacancy and excited-electron states in the diagram, including the intermediate ones.

In this work, as the first step of investigation of this rather complicated process, we tried to find a few diagrams whose contribution to the total amplitude dominates because of certain physical reasons, which result in a large numerator or (and) in a small denominator in the equations similar to equation (3).

Large values of Coulomb matrix elements may occur in the case of strong interaction between the intermediate and the initial or final states. Normally, the Coulomb matrix elements are large if they involve two or more identical one-electron wavefunctions. If additionally at least one of the energy denominators (which is called virtuality) in equation (3) is small when the intermediate state belongs to the discrete spectrum, then strong mixing of these states occurs and the contribution of the diagram to the total amplitude may dominate over others (see, e.g. figure 3(b)).

The contribution of a diagram can also be large if the singularity in equation (3) is in the continuous spectrum. Then the corresponding diagram describes a real multi-step process, which can proceed if allowed by energy and angular momentum

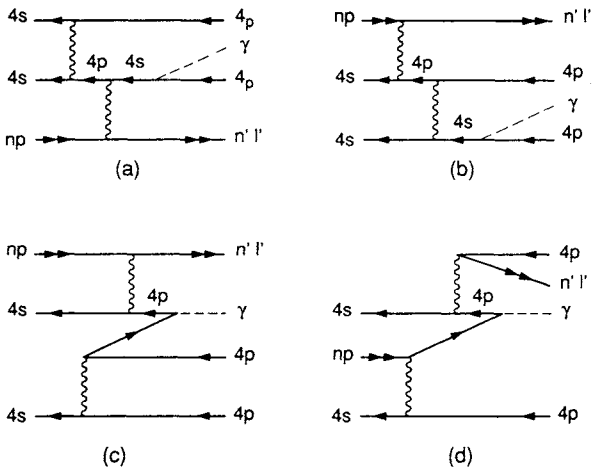

Figure 3. The perturbation theory TERT diagrams included in the present calculation of the transition $4s^{-2}np \rightarrow 4p^{-2}n'l' + \gamma$. Note that the other-time-version diagrams for the two Coulomb interactions in (*c*) and (*d*) were also included, as well as all the exchange diagrams for (*a*)-(*d*).

conservation laws. For example, figure 3(*d*) stands for the autoionization transition $4s^{-2}np \rightarrow 4s^{-1}4p^{-1} + e$ followed by the Auger-type 'transition' $4s^{-1}4p^{-1} \rightarrow 4p^{-3}n'l'$. Finally, the radiative annihilation of the intermediate Auger electron e and the 4p vacancy takes place. The contribution of equation (3) at the point of singularity ε_0 in the continuum is defined by the value of the integrand at this point, e.g. $\langle i_1 i_2|u|j\varepsilon_0\rangle\langle\varepsilon_0 n'|u|f_2 n\rangle\langle j|\boldsymbol{D}|f\rangle/(\varepsilon_{i_1} + \varepsilon_{i_2} - \varepsilon_k - \varepsilon_0)$, if $\varepsilon_j - \varepsilon_{f_1} + \omega = 0$.

The final expressions for the partial TERT amplitudes A_p suitable for a real calculation are obtained in a standard manner (Amusia *et al* 1993) using equation (3), so that orbital, spin and radial parts of amplitudes have been separated. The orbital and spin factors consist of a 6-*j* Wigner coefficient product. They automatically contain angular momentum selection rules for TERTs. The final formulae are not presented here because of their rather complicated structure.

In the specific example of TERTs $4s^{-2} \rightarrow 4p^{-2}n'l' + \gamma$ the diagrams of figure 3 have been found to satisfy quite well the conditions mentioned above. Only these diagrams were included into the calculation. The wavefunctions of the excited electrons, involved in matrix elements of the partial amplitudes A_{a-d}, were calculated in the field of electron configurations as presented in a corresponding diagram in figure 2. For example, the wavefunctions of $n'l'$ electrons were obtained in the self-consistent field of the final ion core $4p^{-2}$. The experimental energies (Striganov and Sventitskii 1968) of the initial, final and intermediate states were employed in calculations of the emitted photon energies and virtualities.

As it was stated above, the TERT $4s^{-2}np \rightarrow 4p^{-2}n'l' + \gamma$ is possible if an excited electron *n*p changes orbital momentum $l = 1$ to $l' = 0, 2$, thus being an active participator in a transition. The various principle quantum numbers $n' = 4, 5, 6, \ldots$ of the excited electron in the final configurations $4p^{-2}[LS]n'l'[L'S']$ of different energies result, in turn, in the emitting of photons of different energies.

Table 1 lists the most probable TERTs $4s^{-2}n \rightarrow 4p^{-2}n'l'$, as well as the energies of the emitted photons. Other TERTs are also possible according to the established selection rules.

Table 1. Photon energies (eV) and partial widths (10^{-7} eV) of the three-electron radiative transitions $4s^{-2}np \rightarrow 4p^{-2}n'l'$.

Final state $4p^{-2}[L_1S_1]n'l'[LS]$	$np = 5p$		$np = 6p$	
	ω (eV)	W (10^{-7} eV)	ω (eV)	W (10^{-7} eV)
^1S 5s ^2S	30.07	0.57	37.72	0.07
6s	27.76	0.07	31.41	0.09
4d ^2D	26.82	0.49	30.48	0.06
^1D 5s ^2D	32.32	3.45	35.96	0.51
6s	27.00	0.37	30.65	0.71
4d ^2P	29.30	0.91	32.95	0.10
5d	26.05	0.24	29.70	0.07
4d ^2D	29.58	1.17	33.21	0.13
5d	26.15	0.33	29.85	0.09

It is seen that the most probable transitions are those by which the excited electron np either does not change its principle quantum number n, while its orbital momentum decreases ($np \rightarrow ns$), or changes it to a lower value, while the orbital momentum increases ($np \rightarrow (n-1)d$). The transition probabilities to the ^2D final states are larger due to the large statistical weight. Although the transition probabilities from the initial $4s^{-2}6p$ state are approximately ten times smaller than those from $4s^{-2}5p$, the largest ones from $4s^{-2}6p$ compete with some of the transitions from $4s^{-2}5p$.

The calculations of the partial amplitudes showed that the main contribution to the probability of TERTs $4s^{-2}np \rightarrow 4p^{-2}n'l'$ is given by term A_b (figure 2(b)) in which a part of correlations within the core and excited electron subshells is taken into account. The others are either small or significantly compensate each other because of opposite signs of the virtualities.

The results obtained in our calculations demonstrate the rather high probability of the TERTs with partial widths of the order 10^{-7} to 10^{-8} eV. These values are of the same order as, e.g., the probabilities of some satellite transitions or single-photon decays of double-hole states (Amusia *et al* 1977a, b).

In order to compare the calculated TERTs width with the present experimental data, the total width of 0.14–0.18 eV of the $4s^{-2}5p$ state, populated by the Auger-like transition $3d^{-1}5p \rightarrow 4s^{-2}5p$ with the partial width of 3×10^{-3} eV, has to be taken into account (Amusia *et al* 1993). Then, with respect to the decay of the $3d^{-1}5p$ resonance, the upper limit of theoretical width estimation is equal to $3 \times 10^{-3}\,\text{eV} \times 3.45 \times 10^{-7}\,\text{eV}/0.14\,\text{eV} \sim 7 \times 10^{-9}$ eV.

The new lines, observed in the PIFS experiment, were found to be approximately 40 times weaker than the main $4s^{-1} \rightarrow 4p^{-1}$ line, which has a cross section of 0.2 Mb (Aksela *et al* 1987), so that a typical cross section for the new lines observed is 0.005 Mb. The above theoretical partial width estimation of 7×10^{-9} eV has to be divided by the total width of 83 meV (King *et al* 1977) and multiplied by the cross section of 3.5 Mb (Lablanquie and Morin 1991) of $3d^{-1}5p$ resonance in order obtain the upper limit of the theoretical cross section which amounts to $\sim 3 \times 10^{-7}$ Mb. This cross section is at least four orders of magnitude smaller than the one of the observed lines.

These estimations show that in order to observe the TERTs, the experimental sensitivity must be increased by a factor of 10^4 or more, at least in the case of $4s^{-2}np \rightarrow 4p^{-2}n'l'$ radiative transitions. Furthermore, the results obtained demonstrate

that the initial states of the fluorescence decay process to be observed must not possess large non-radiative partial widths with respect to the radiative ones. On the other hand, current studies suggest that the new observed lines are due to transitions in Kr III. The results of these investigations will be presented in a forthcoming paper.

It was demonstrated here that a new kind of correlative decay, namely three-electron radiative transitions, should take place with a reasonably high probability. The relative role of different kinds of interelectron correlations, leading to the decay process, was examined and clarified. Concrete results were obtained for the Kr II transitions $4s^{-2}np \rightarrow 4p^{-2}n'l' + \gamma$. Closely connected to the considered process is another one in which not only a photon but also an Auger-type electron could be emitted, e.g. the transition $4s^{-2}np \rightarrow 4p^{-2} + e + \gamma$. This type of correlative transition leads not only to discrete photon and electron lines in spectra, but is also responsible for the continuous spectrum of electrons and photons whose observation in coincidence would be of interest, too.

LVC and VAK would like to thank the Department of Physics, University of Kaiserslautern for the possibility of working during their stay in Germany. MYA is grateful to the Alexander von Humboldt-Stiftung, which made his staying and researching in Frankfurt/Main, Germany, possible. Technical support by the staff of BESSY is gratefully acknowledged. This work has been funded by the German Federal Minister for Research and Technology under contract nos 05 452AXI 5 and 05 5UKAXB.

References

Aksela S, Aksela H, Levasalmi M, Tan K H and Bancroft G M 1987 *Phys. Rev.* A **36** 3449–50

Amusia M Ya and Chernysheva L V 1983 *Automation System for Atomic Structure Research* (Leningrad: Nauka) (in Russian)

Amusia M Ya, Kilin V A, Ehresmann A, Schmoranzer H and Schartner K H 1993 *J. Phys. B: At. Mol. Opt. Phys.* submitted for publication

Amusia M Ya, Kilin V A, Kolesnikova A N and Lee I S 1977a *JETP* **57** 1246 (in Russian)

Amusia M Ya, Lee I S and Zinoviev A N 1977b *Phys. Lett.* **60A** 172

Ehresmann A, Kilin V A, Amusia M Ya, Vollweiler F, Schmoranzer H, Moebus B, Mentzel G and Schartner K H 1992 *Proc. 10th Int. Conf. on VUV Radiation Physics (Paris)* ed Y Petroff, I Nenner and F Wuilleumier Abstracts p TU 62

King G C, Tronc M, Rad F H and Bradford R C 1977 *J. Phys. B: At. Mol. Phys.* **10** 2479

Lablanquie P and Morin P 1991 *J. Phys. B: At. Mol. Opt. Phys.* **24** 4349

Schartner K H, Lenz P, Moebus B, Magel B, Schmoranzer H and Wildberger M 1990 *Phys. Scr.* **41** 853

Striganov A R and Sventitskii N S 1968 *Table of Spectral Lines of Neutral and Ionized Atoms* (New York: Plenum)

Woefli W, Stoller Ch, Bonani G, Suter M and Stoeckli M 1975 *Phys. Rev. Lett.* **35** 656